

The impact of recycled plastic fibers on bending behavior of green RC beams in the sea conditions

Hamed Safayenikoo^{1*}, Hamid Shahrabadi²

^{1*} Civil Engineering Department, Marine Engineering School, Chabahar Maritime University, Chabahar, Iran; hamed.safayenikoo@gmail.com

² Civil Engineering Department, Marine Engineering School, Chabahar Maritime University, Chabahar, Iran; hamid.shahrabadi@gmail.com

ARTICLE INFO

Article History:

Received: 1 Oct 2024

Accepted: 11 Jun 2025

Keywords:

Disposable Glasses Fiber
Garbage Bag Fiber
Green Reinforced Concrete
Metakaolin and Zeolite
Flexural and Cracking Behavior

ABSTRACT

Marine concrete structures, due to proper mechanical behavior and high durability for the world population, which are directly or indirectly related to marine infrastructure and various industries seem essential. On the other hand, concrete production and other related industries in marine environments are the main agents of production of pollution and waste and excessive consumption of the earth's natural resources and energy. Therefore, it seems that the simultaneous use of cement replacements to reduce the generation of greenhouse gases derived from cement production and plastic waste as fiber can decrease environmental pollution and improve concrete mechanical behavior. This study investigates the impact of incorporating 0.5 and 1% strip disposable glass fibers (GF) and strip garbage bag fibers (BF) on the flexural and cracking characteristics of reinforced concrete (RC) beams containing 10% metakaolin/zeolite. The investigation is conducted over 28 and 180 days in the tidal environment of the Oman Sea. Considering the results, by adding GF and BF to the green RC beams the flexural toughness (T) increased up to 47 and 27%, respectively. Furthermore, the cracking load (P_{cr}) of glass fibers RC (GC) and bags fibers RC (BC) beams was lower than RC up to 32 and 21%, respectively. Moreover, the incorporation of GF and BF resulted in an increase of up to 28% and 16% in the maximum load capacity (P_{max}) of RC beams, respectively. In addition, the P_{max} and T of GC beams were higher than BC. Besides, it was observed that metakaolin GC and BC beams exhibited a greater value of P_{max} and T compared with zeolite beams.).

1. Introduction

The importance of the sea and its related industries, and sustainable human access to food, industrial, and energy resources, has caused an increase in maritime regions' human population [1], [2]. Therefore, there is a greater human demand for building coastal and offshore infrastructure. Hence, concrete, which is a mixture of readily available and cheap raw materials, can be the best choice for the construction of marine structures [3], [4], [5], [6]. Furthermore, based on the environmental conditions of sea, concrete with high durability and suitable strength can increase the service life of marine structures. However, excessive consumption of irreversible primary resources, generation of air and marine pollution (produce less than 1 ton of CO₂ greenhouse gas per 1 ton of

cement), low tensile force, and ductility are the most important weaknesses of concrete [1], [3], [7], [8], [9]. The supplementary cementitious materials (SCMs) like metakaolin and zeolite can be used to reduce the generation of environmental pollution and energy consumption [1], [3].

Metakaolin is a material characterized by its smaller particle size compared to cement and its significant pozzolanic reactivity. It is produced through the process of calcination, wherein kaolin is heated to temperatures ranging from 600 to 900 °C, without producing CO₂, in a specified time. Moreover, the mechanical and durability characteristics of mixes by substitution of cement with metakaolin are improved [10], [11], [12], [13]. Kavitha et al. found that substituting cement with metakaolin in self-

compacting concrete (SCC) mixes enhanced the compressive (f'_c) and tensile (T_c) strengths [14]. Furthermore, Punitha et al. demonstrated that the substitution of 10% of cement with metakaolin in concrete incorporating high-density polyethylene plastic waste resulted in an increase in the f'_c , T_c , and flexural strength of the concrete [15].

On the other hand, zeolite is a material with a regular crystalline structure, porous, and high specific surface area, which has high pozzolanic activity [2], [3], [16]. By using zeolite as an SCM in concrete mixture, the quality of microstructures improved, the mechanical strength increased, and the porosity and permeability of concrete decreased [3], [16], [17], [18]. Najimi et al. reported that the use of zeolite enhanced water and chloride ion penetration while decreasing f'_c and workability [5]. Tran et al. presented that the f'_c and T_c , water permeability, and capillary absorption of concrete mixtures by use of zeolite, were decreased over a long time [7].

As a result, metakaolin and zeolite as SCMs improved concrete mixes' mechanical properties and environmental impact [3], [8], [10], [14], [19], [20], [21]. On the other hand, fine particles and high specific surface area in SCMs increase chemical activities, produce more heat, and finally, cause cracking in the mixtures. Cracks' appearance in concrete structures, especially in marine environments are the main cause of chemical ions attacking and deterioration [22], [23]. Therefore, using different types of fibers can prevent and reduce cracking and limit crack propagation. Moreover, the incorporation of fibers into concrete mixes has the potential to enhance resistance parameters, including flexural behavior and ductility [8], [22], [23], [24], [25]. On the other hand, by recycling, incorporating waste fibers into concrete mixes, and generating green concrete, environmental pollution from landfilling and incineration will be reduced [26], [27]. Green concrete is an environmentally friendly concrete that uses waste, residual or recycled materials or requires less energy consumption due to SCMs use in concrete. Based on environmental conditions and the application type of concrete structure, different types of fibers, like synthetic and recycled synthetic fiber in concrete are utilized [27], [28], [29], [30].

Alabduljabbar et al. concluded that green concrete using recycled polypropylene fibers and palm oil fuel ash (POFA) showed greater flexural strengths and T than control specimens while having less drying shrinkage and workability [29]. Song et al. found that the incorporation of nylon and polypropylene fibers in concrete resulted in increased values of f'_c , T_c , modulus of rupture, and impact resistance compared to plain concrete [9]. In addition, Yap et al. reported that the flexural strengths, T_c , and f'_c of the concrete by adding polypropylene, nylon, and oil palm shells fibers will be increased [27].

Kim et al. discovered that by using beverage container fibers in concrete mixes, the flexural behavior and ductility increased while the f'_c , modulus of elasticity, and drying shrinkage were reduced [26]. Also, according to Alani et al. strip fibers from PET bottle waste and POFA enhanced the f'_c , porosity, and chloride permeability of ultra-high-performance green concrete [30]. In another study, Ahdal et al. showed that the f'_c of green concrete samples containing 10% zeolite and 1% PET fibers increased than plain concrete [28].

According to this background and little research has been done, it seems that fibers and SCMs in green concrete mixes may reduce pollutants and improve maritime concrete structures' mechanical properties, ductility, and durability. Thus, in current research, the impact of various types and amounts of GF and BF on flexural capacity, T , cracking behavior, and microstructure of green RC beams that incorporate metakaolin and zeolite in Oman Sea conditions, will be investigated.

2. Experimental Program

2.1 Materials

Portland cement (Type II), metakaolin or zeolite, aggregate (fine and coarse), water, superplasticizer, and GF and BF were used. The concrete mixtures were made with Kerman industrial cement. In all concrete mixtures, metakaolin or zeolite replaced 10% of the cement weight (Figure 1). Cementitious materials' chemical and physical properties are shown in Tables 1 and 2 [31].



Figure 1. The binders

Table 1. Binder's physical properties [31]

	Cement	Metakaolin	Zeolite
Specific gravity	3.15	2.45	2.18
Surface area (m ² /kg)	310	1200	320

Table 2. Binder's chemical composition [31]

Combination (%)	Cement	Metakaolin	Zeolite
Calcium oxide	63.52	1.34	7.38
Silica dioxide	21.50	81.29	58.15
Aluminum oxide	4.95	11.32	8.18
Iron oxide	3.97	0.56	1.54
Magnesium oxide	1.75	0.59	3.92
Potassium oxide	0	0.82	0.82
Sodium oxide	0	1.04	1.11

Titanium oxide	0	0.107	0.175
Manganese oxide	0	0.003	0.019

The Chabahar mines were utilized to prepare fine and coarse aggregates with maximum diameters of 4.75 and 19 mm, respectively. Figure 2 showed the sieve analysis of aggregates as per the guidelines of ASTM C136 [32].

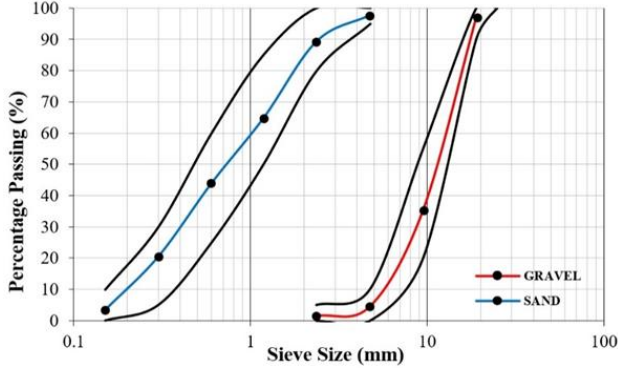


Figure 2. The sieve analysis of aggregates [32]

Table 3. The aggregates' characteristics [31]

Aggregate	Water absorption (%)	Specific gravity
Sand	2.92	2.64
Gravel	1.84	2.42

In the laboratory, potable water was utilized for the preparing and curing (in primary ages) of all concrete mixes. Conversely, the utilization of both SCMs and fibers in concrete mixtures has led to the use of Farco Plast, a modified polycarboxylate-based superplasticizer, for regulating the concrete's workability. In Table 4, the main characteristics of Farco Plast are shown.

Table 4. The Farco Plast superplasticizer properties [31]

Physical state	Color	Specific gravity
Liquid	Light Brown	1.09 (kg/Lit)



Figure 3. Drinking water curing tanks [31]

The recycled strip fibers used in mixtures (hereafter named strip fibers) were prepared by cutting polyethylene disposable glasses and garbage bags. The V_f of fibers utilized in the production of blends was determined to be 0.5 and 1%. Furthermore, for fibers with a rectangular section, the fiber aspect ratio (A.R.) formula was:

$$\lambda = \frac{l}{d_e} = \frac{l}{2 \times \sqrt{\frac{A}{\pi}}} = \frac{l}{2 \times \sqrt{\frac{b \times c}{\pi}}} \quad (1)$$

Where λ is A.R., l is fiber length (mm), d_e is equivalent diameter (mm), A is fiber cross-section area (mm²), b is fiber width (mm) and c is fiber thickness (mm) [33]. For desired strength performance of mixtures, an A.R. of fiber more than 20 is required [34].

Table 5. The fiber properties [31]

Strip Fibers	No	Width (mm)	Thickness (mm)	Length (mm)	Aspect Ratio	Density (kg/m ³)	Tensile Strength (MPa)
Disposable Glasses (G)	G1	10	0.03	25	≈ 40	≈ 680	≈ 570
	G2	10	0.03	50	≈ 80	≈ 680	≈ 570
Garbage Bags (B)	B1	10	0.03	25	≈ 40	≈ 570	≈ 52
	B2	10	0.03	50	≈ 80	≈ 570	≈ 52



Figure 4. Strip fiber types: A) GF [31], B) BF

2.2. Concrete Mixtures

In this study, 18 green RC mixtures were prepared. Throughout all concrete mixes, the W/B was always kept at 0.5. There were 410 kg/m³ of binders in all concrete mixtures. Moreover, the Farco plast superplasticizer was used at up to 2% of cement weight to control and improve concrete workability. Table 6 illustrates the concrete composition [31].

2.3. Preparation of samples

Following the preparation and measurement of the materials, a rotary mixer was employed to blend them. After the completion of the task, the diverse varieties of fibers were incorporated into the homogeneous mixture of concrete and blended for a short time. Subsequently, concrete mixes, based on the type of test, were cast in the relevant molds. Following 24 hours, the molds were extracted and the samples were transferred to tanks containing potable water for a curing duration of three days. Finally, the specimens were transferred to the Oman Sea's tidal zone and left to acclimate for a duration ranging from 28 to 180 days. The number of cubes (150 mm for f'_c) and beams (150×150×650 mm for four-point bending tests) was 54 and 72, respectively. On the other hand, for concrete microstructure analyses, 52 cubes (70 mm) were prepared.

Table 6. The concrete composition [31]

Mix	Sand (kg/m ³)	Gravel (kg/m ³)	Water (kg/m ³)	Binders (kg/m ³)			Strip Fibers (kg/m ³)			
				Cement (C)	Metakaolin (Mk)	Zeolite (Ze)	Garbage Bag		Disposable Glass	
							B1	B2	G1	G2
1	NF1				41	---	---	---	---	---
2	NF2				---	41	---	---	---	---
3	B1				41	---	2.85	---	---	---
4	B2				41	---	---	2.85	---	---
5	B3				---	41	2.85	---	---	---
6	B4				---	41	---	2.85	---	---
7	B5				41	---	5.7	---	---	---
8	B6				41	---	---	5.7	---	---
9	B7	664	1054	205	369	---	41	5.7	---	---
10	B8					---	41	---	5.7	---
11	G1				41	---	---	---	3.4	---
12	G2				41	---	---	---	---	3.4
13	G3				---	41	---	---	3.4	---
14	G4				---	41	---	---	---	3.4
15	G5				41	---	---	---	6.8	---
16	G6				41	---	---	---	---	6.8
17	G7				---	41	---	---	6.8	---
18	G8				---	41	---	---	---	6.8

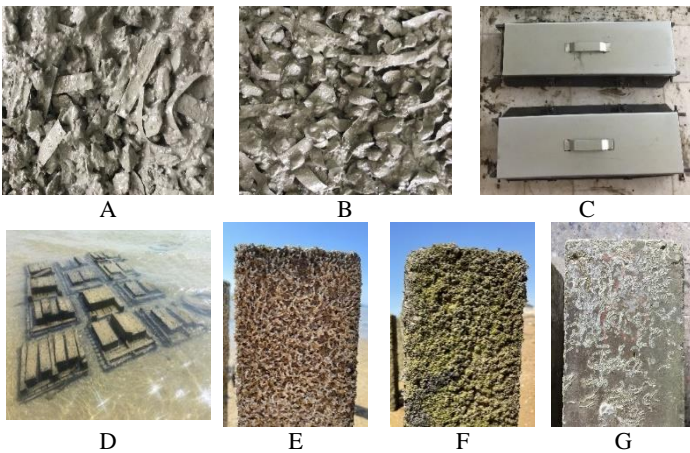


Figure 5. A) The GC, B) The BC, C) Specimen's molds, D) Samples in the coastal zone, E and F) Samples collected from the Oman Sea, G) Samples after preparing for tests [31]

The GC/BC beams were made utilizing steel bars ($f_y=400$ MPa and $f_u=600$ MPa) with diameters of 8 mm and 6 mm for the longitudinal reinforcements and stirrups. Figure 6 illustrated the specifics of GC/BC beams [31].

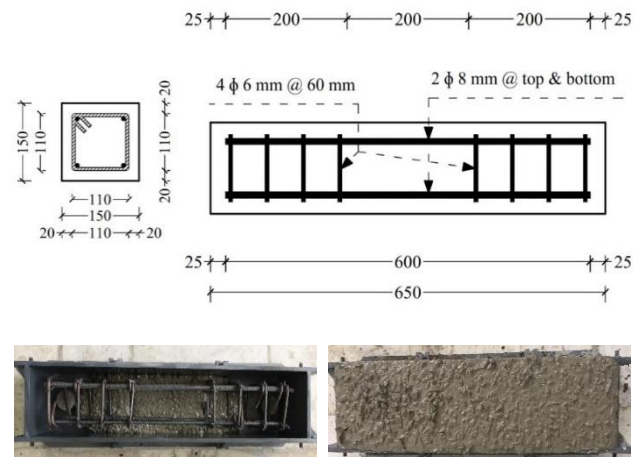


Figure 6. The GC/BC beam [31]

2.4. Exposure conditions

In this research, due to consider the most destructive effects of sea environment on concrete structures, the specimens were exposed to a 180-day exposure period in the Oman Sea's tidal zone. Figure 5 demonstrated the state of the concrete samples located on the shoreline of the Oman Sea. Also, Table 7 presents the chemical characteristics of both laboratory and Oman seawater [31].

Table 7. The chemical properties of water (gr/Lit) [31]

	PH	Hardness	Alkalinity	SO₄²⁻	NO₂⁻	NO₃⁻	Cl⁻	Ca	Mg	NH₃	Zn	Al	Cu	Mn	Fe
Lab-water	6.70	45	20	102	0.010	2.820	5	4	≈0	≈0	≈0	0.32	0.02	0.004	≈0
Seawater	7.97	225	120	≈0	0.007	0.222	5	68	95	1.29	0.22	0.32	0.02	≈0	0.04

3. Testing methods

3.1 Compressive strength (f'c)

The BS EN12390-3 standard measured the f'c value by exposing three 150×150×150 mm cubic specimens for 28 days in the Oman Sea's tidal zone. By averaging three specimens, the concrete mixture's f'c was computed [35].

3.2 Flexural behavior

The ASTM C78 standard's four-point bending test was used to evaluate the flexural behavior of concrete beams. A universal testing machine was used, with a constant rate of 100 N/s [36]. During the loading process, the deformation of the beams was recorded by a mobile camera and computer. Based on the recorded information, the behavior and characteristics of beam cracks were investigated. Moreover, the maximum deflection of mid-span for beams was terminated to 20 mm [31].

In the following, the load-deflection curve for various types of GC/BC beams was drawn and then some characteristics of flexural behavior of beams such as Pcr, Pmax, and T were calculated. Moreover, flexural toughness was calculated by integrating the load-deflection curve.

4. Results and Discussions

4.1. Specific gravity (γ)

The γ of green concrete, both with and without fibers, is presented in Figure 7. Also, Table 8 compares the influence of fiber types on the γ of concrete samples.

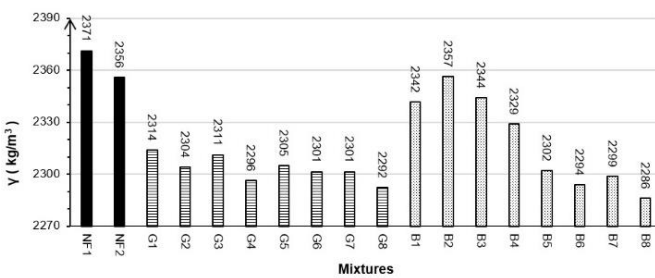


Figure 7. The green concrete's specific gravity (γ)

Table 8. Comparison of specific gravity (γ) at 28 days

Mix	γ	Mix	γ	Mix	γ	Mix	γ
NF1	1	NF2	1	NF1	1	NF2	1
G1	0.976	G3	0.981	B1	0.988	B3	0.992
G2	0.972	G4	0.975	B2	0.984	B4	0.989
G5	0.972	G7	0.977	B5	0.971	B7	0.976
G6	0.970	G8	0.973	B6	0.967	B8	0.970

The results show that fibers in green concrete mixes reduce the γ of concrete. Moreover, by increasing the Vf of fibers in mixes, the γ decreased more. At 28 days, the γ of concrete with 0.5% GF was observed to be higher than that of concrete with 0.5% BF.

However, increasing the Vf of fibers up to 1% resulted in equal γ for both types of fibers. It seems that adding fibers and augmentation of Vf within mixes resulted in an increase in the volume of pore space and porosity, while concurrently leading to a decrease in γ [2], [28], [37], [38], [39], [40], [41], [42], [43].

4.2. Compressive strength

In Figure 8 and Table 9, the results of f'c in different mixtures containing various types of strip fibers and SCMs are shown at 28 days.

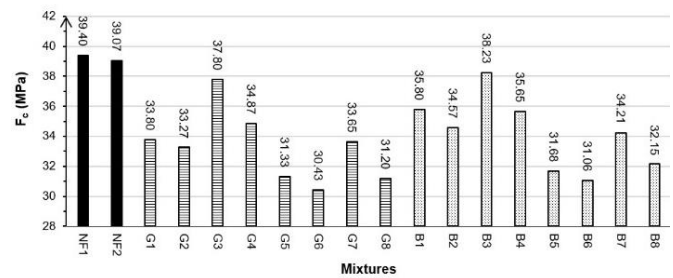


Figure 8. The f'c of specimens

Table 9. Comparison of f'c

Mix	f'c	Mix	f'c	Mix	f'c	Mix	f'c
NF1	1	NF2	1	NF1	1	NF2	1
G1	0.86	G3	0.97	B1	0.91	B3	0.98
G2	0.84	G4	0.89	B2	0.88	B4	0.91
G5	0.80	G7	0.86	B5	0.80	B7	0.88
G6	0.77	G8	0.80	B6	0.79	B8	0.82

By comparing the results, it is evident that the combining of fibers and augmentation of the Vf in green concrete led to a rise in the volume of pore space, thereby causing a reduction in the density, adhesion between fibers and cement paste, integrity, and f'c. Similarly, through the augmentation A.R. and dimensions of fibers in mixtures, porosity increased but adhesion and f'c decreased [44], [45], [46], [47], [48], [49], [50], [51], [52]. Adding 0.5 and 1% GF resulted in a reduction of up to 16 and 23% in the f'c of the green concrete specimens, respectively. While concrete samples containing 0.5 and 1% BF had lower f'c than simple ones about 12 and 21%, respectively.

In contrast, it was noted that the f'c of concrete samples with 0.5% BF was greater than that of those containing 0.5% GF. However, the addition of 1% BF or GF fibers to plain concrete resulted in equivalent f'c values among the specimens.

The enhanced flexibility of BF in comparison to GF has improved the homogeneity and integrity of the concrete. Conversely, GF mixtures exhibited higher porosity, leading to reduced fiber-cement paste adhesion, ultimately resulting in a lower f'c [9], [23], [27], [44], [49], [50], [51], [53], [54], [55].

Furthermore, at 28 days, in mixtures with an equal amount of fiber, f'_c of metakaolin concrete specimens had up to 12% lower than zeolite ones. The hydrophilic structure of zeolite appears to result in heightened water absorption and reduced workability, decreasing concrete porosity and increasing f'_c [7], [22], [25], [56], [57].

4.3. Flexural behavior

After four-point bending test on RC and fiber RC beams at 28 and 180 days, flexural properties consisting of P_{cr} , P_{max} , T , and cracking behavior were examined. The flexural properties are demonstrated in Tables 10-12.

Table 10. Four-point bending test results

Mixes	P_{cr} (kN)		ΔP_{max} (mm)		P_{max} (kN)		T (kN.m)	
	28	180	28	180	28	180	28	180
N1	28.40	37.20	4.04	4.53	80.15	90.5	1133.41	1250.62
N2	27.10	36.20	3.86	4.36	71.9	84.2	1035.07	1210.24
G1	22.10	28.87	6.18	6.48	89.6	104.2	1432.09	1594.07
G2	24.40	30.88	7.64	7.76	97.8	115.6	1601.39	1785.50
G3	21.41	29.83	5.86	6.16	80.4	96.6	1261.13	1493.18
G4	22.17	32.29	6.46	6.72	88.7	107.6	1425.28	1707.09
G5	20.16	25.37	6.78	7.02	84.9	99.0	1499.22	1671.75
G6	21.07	27.08	8.32	8.48	94.3	108.9	1648.13	1842.20
G7	18.67	26.06	6.08	6.38	76.3	90.8	1326.87	1568.42
G8	19.35	27.87	7.12	7.32	83.5	101.7	1460.39	1745.28
B1	25.21	34.32	4.96	5.56	82.6	95.1	1223.72	1358.53
B2	26.56	36.42	5.94	6.64	87.6	100.4	1303.67	1450.88
B3	23.88	33.98	4.74	5.32	76.4	92.2	1114.17	1323.39
B4	25.17	35.78	5.16	5.78	80.8	97.2	1202.41	1413.93
B5	23.02	29.51	5.36	6.00	80.6	92.8	1304.35	1475.84
B6	23.87	31.02	6.42	7.16	84.6	96.8	1426.25	1581.67
B7	21.07	30.44	4.88	5.48	73.4	88.6	1188.51	1393.77
B8	22.01	32.01	5.60	6.26	78.8	94.6	1287.14	1508.75

ΔP_{max} : Mid-span deflection of beams at P_{max}

Table 11. Comparison of P_{cr} for beams

Age	Mix	P_{cr}	Mix	P_{cr}	Mix	P_{cr}	Mix	P_{cr}
28	G1	0.778	G3	0.790	B1	0.888	B3	0.881
	G2	0.859	G4	0.818	B2	0.935	B4	0.929
	G5	0.710	G7	0.689	B5	0.811	B7	0.777
	G6	0.742	G8	0.714	B6	0.841	B8	0.812
	NF1	1	NF2	1	NF1	1	NF2	1
180	G1	0.776	G3	0.824	B1	0.923	B3	0.939
	G2	0.830	G4	0.892	B2	0.979	B4	0.988
	G5	0.682	G7	0.720	B5	0.793	B7	0.841
	G6	0.728	G8	0.770	B6	0.834	B8	0.884
	NF1	1	NF2	1	NF1	1	NF2	1

4.3.1. The GC beams' load-deflection behavior

Figures 9–12 illustrate the load-deflection curves for GC and RC beams incorporating metakaolin or zeolite.

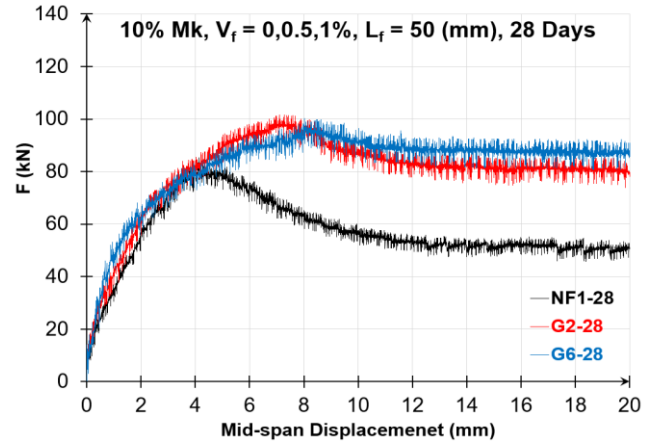
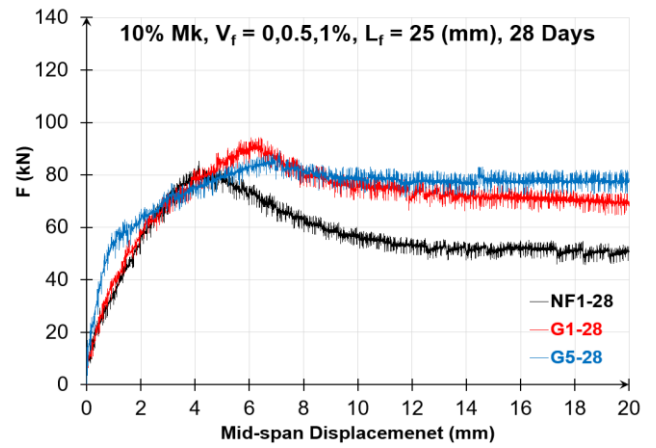


Figure 9. Metakaolin GC beam load-deflection curve

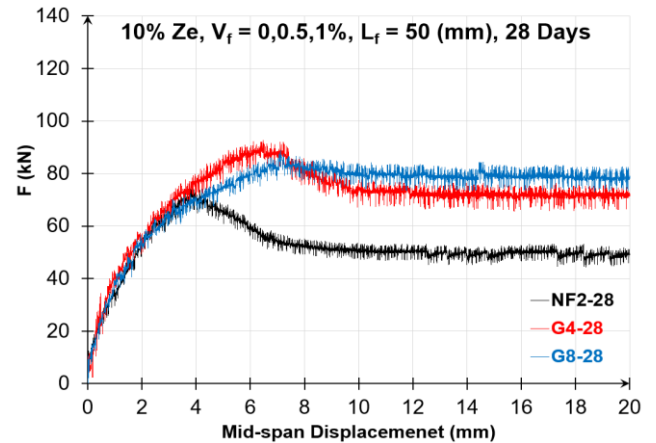
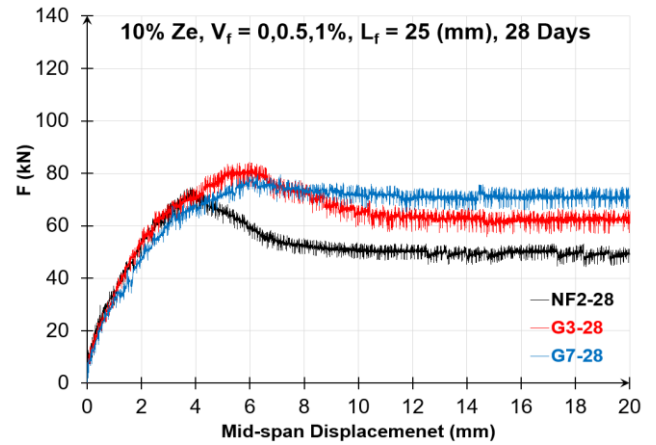


Figure 10. Zeolite GC beam load-deflection curve

Table 12. Comparison of P_{max} and T of RC beams

Age	Mix	P_{max}	T	Mix	P_{max}	T	Mix	P_{max}	T	Mix	P_{max}	T
28	NF1	1	1	NF2	1	1	NF1	1	1	NF2	1	1
	G1	1.118	1.264	G3	1.118	1.218	B1	1.031	1.080	B3	1.063	1.076
	G2	1.231	1.413	G4	1.234	1.377	B2	1.093	1.150	B4	1.124	1.162
	G5	1.059	1.323	G7	1.061	1.282	B5	1.007	1.151	B7	1.021	1.148
	G6	1.177	1.454	G8	1.161	1.411	B6	1.056	1.258	B8	1.096	1.244
180	NF1	1	1	NF2	1	1	NF1	1	1	NF2	1	1
	G1	1.151	1.275	G3	1.147	1.234	B1	1.051	1.086	B3	1.095	1.093
	G2	1.277	1.428	G4	1.278	1.411	B2	1.109	1.160	B4	1.154	1.168
	G5	1.094	1.337	G7	1.078	1.296	B5	1.025	1.180	B7	1.052	1.152
	G6	1.203	1.473	G8	1.208	1.442	B6	1.070	1.265	B8	1.124	1.247

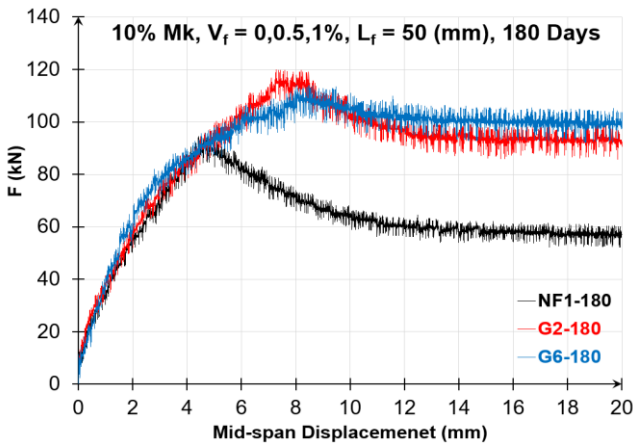
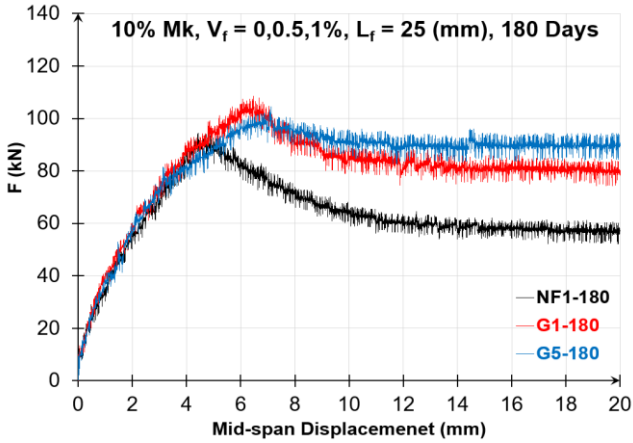


Figure 11. Metakaolin GC beam load-deflection curve

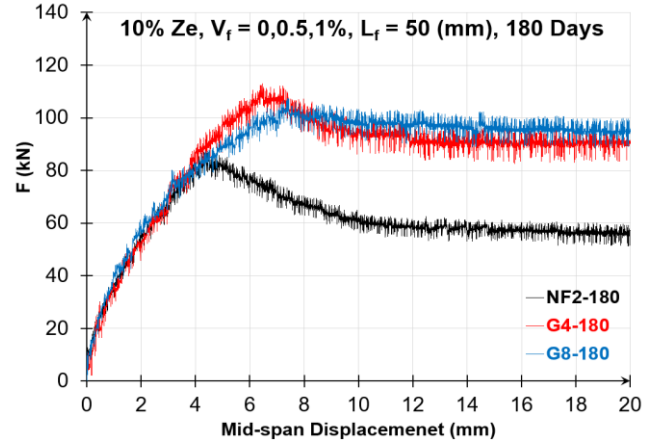
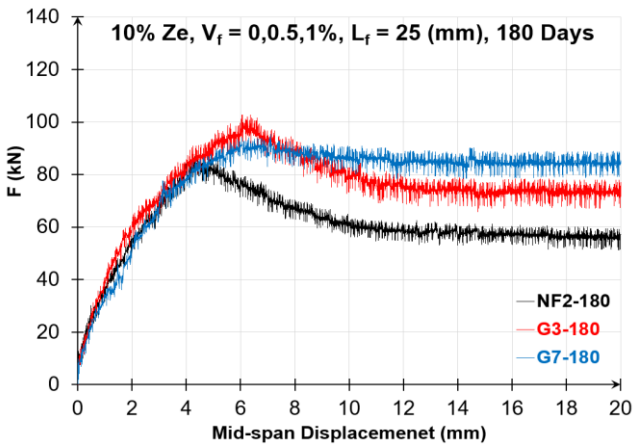


Figure 12. Zeolite GC beam load-deflection curve

4.3.1.1. The GC beam cracking load

In Tables 10-11 and Figure 13, the P_{cr} of GC beams are presented and compared at 28 and 180 days.

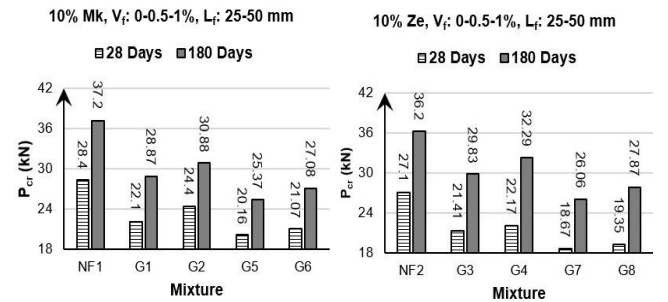


Figure 13. The Cracking load

Based on the result, the P_{cr} was reduced when 0.5 and 1% GF were added to metakaolin/zeolite RC beams at all ages. By combining 0.5 and 1% GF to metakaolin RC beams after 28 days, the P_{cr} dropped by 22 or 29%, respectively. Moreover, depending on whether the beams included 0.5 or 1% GF, the P_{cr} of the metakaolin GC beams after 180 days was 24 and 32% lower than RC beams. Besides, the P_{cr} of the zeolite GC beams was 21 and 31% lower than RC beams at 28 days, respectively, based on that the beams included 0.5 or 1% GF. At 180 days, the P_{cr} was reduced by either 0.5 or 1% GF when added to RC beams, respectively. According to the results, it seems that by adding GF to RC beams, pores in cement matrixes and porosity are increased which may lead to

a decrease in cohesion and the P_{cr} [15], [26], [55], [58], [59], [60], [61].

Conversely, the GC beams P_{cr} was enhanced by augmentation of the GF A.R. For instance, in 10% metakaolin/zeolite GC beams and 0.5 and 1% GF, the P_{cr} demonstrated an increase, reaching a maximum of 6 and 9% for A.R. of 40 and 80, respectively. The enhancement of adhesion and bonding length in the cement matrix can be achieved by increasing the A.R. of fibers. As a result, it is feasible to enhance the fiber's resistance to extraction and the occurrence of cracks in beams [33], [48], [62].

Results and Figures 9-12 reveal that the P_{cr} of GC beams including metakaolin was approximately 10% greater than those of zeolite, after a curing period of 28 days. Also, the P_{cr} of Zeolite GC beams exhibited a similar trend to that of the Metakaolin at long time [8], [16], [31], [60].

4.3.1.2. The GC beams peak load

Based on the data displayed in Table 12 and Figure 14, it is evident that an increase in the V_f of GF in the metakaolin/zeolite GC beams resulted in a decrease in P_{max} at all days.

The P_{max} of GC beams was greater than that of RC beams, nevertheless. For instance, the addition of 0.5 and 1% GF to the RC beams resulted in a significant increase in P_{max} by 23 and 18%, respectively, within a brief period. Moreover, GC beams with 0.5 and 1% GF had P_{max} 28 and 21% greater than RC beams after 180 days. Focusing on the obtained findings, it can be concluded that by increasing porosity and reducing the integrity of concrete, which occurs due to the increase of volume fraction in the mixtures, the P_{max} decreases [23], [30], [53], [59], [62], [63].

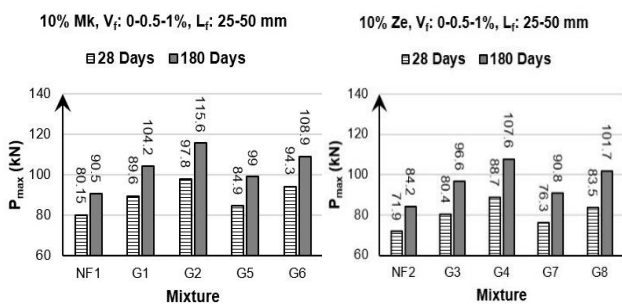


Figure 14. P_{max} of the GC beams

On the other hand, it was observed that the P_{max} of the GC beams enhanced on all days as the A.R. of the GF was increased. For example, the P_{max} values of G2/G8 beams having an A.R. of 80 were 11% greater than those of G1/G7 beams having an A.R. of 40, across all observed days. The length and aspect ratio of GF seems to increase fiber resistance to pull out, slip, and P_{max} [33], [48], [49], [62].

Besides, Table 10 demonstrated that at 28 days, the P_{max} of metakaolin GC beams exceeded that of zeolite GC beams by up to 13%. However, at 180 days, there was a reduction in the disparity between the P_{max}

values of GC beams including metakaolin, and those of zeolite, amounting to approximately 8%.

4.3.1.3. The GC beams flexural toughness

Considering Figures 9-12, 15, and Table 10, obvious that the incorporation of GF into the RC beams resulted in a notable increase in T.

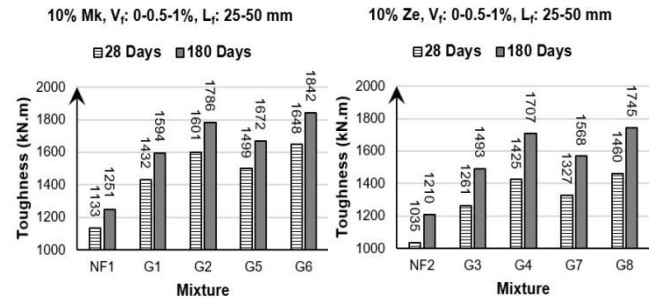


Figure 15. T of the GC beams

The GC beams, which were composed of 0.5 and 1% GF, exhibited significantly higher T values of up to 41% and 45%, respectively, compared to the RC beams after 28 days. While a combination of 0.5 and 1% GF to the RC beams resulted in a respective increase of 43 and 47% for T after 180 days. The bridging phenomenon of GF on the surface and edges of cracks is evidently responsible for the dispersion of the applied loads and constrains the propagation of the initial cracks. Moreover, the V_f of GF in the mixes increased the interfacial bonding between fibers and cement matrix, toughness, and ductility of GC beams [42], [45], [46], [54], [64], [65], [66], [67], [68], [69]. Also, in Figure 16, the crack bridging of GF in bending tests of the GC beams has been presented.



Figure 16. Crack bridging of GF in the GC beams

Based on Table 12, it can be observed that the GC beams with an A.R. of 80 exhibited a higher T value in comparison to those with an A.R. of 40. At 28 days, the T value of the 0.5% GC beams with A.R. of 40 and 80 demonstrated an increase of 27 and 41%, respectively, in comparison to the RC beams. Also, the incorporation of 0.5% GF with A.R. of 40 and 80 resulted in a significant enhancement of the T of RC beams, with an increase of up to 32 and 46% at 180 days, respectively. Furthermore, it was observed that in GC beams with an 80 A.R. and 1% GF content, the highest rise in T, as compared to the 40 A.R., was approximately 11%. The augmentation of length and aspect ratio amplifies both the contact surface and the developmental length of GF. The T of GC beams can be increased by enhancing the adhesion and pull-out

resistance of the cement matrix [28], [43], [45], [47], [54], [58].

On the other hand, it was observed that metakaolin GC beams overtook zeolite ones in T. However, in the long term, zeolite's unique pozzolanic properties reduce the T difference between metakaolin and zeolite in GC beams. The pozzolanic reactivity and finer particles of metakaolin are more effective than that of zeolite, resulting in increased speed of the hydration process. This, in turn, enhances the adhesion between fibers and cement paste, ultimately leading to higher T values at 28 days. However, after 180 days, zeolite outperforms metakaolin due to its ability to produce C-S-H secondary gels, which improve the microstructure of the concrete and accelerate the rate of T growth [8], [10], [13], [16], [22], [25], [31], [38], [60].

4.3.2. The BC beams' load-deflection behavior

Figures 17-20 present the load-deflection curves of the metakaolin or zeolite BC and RC beams.

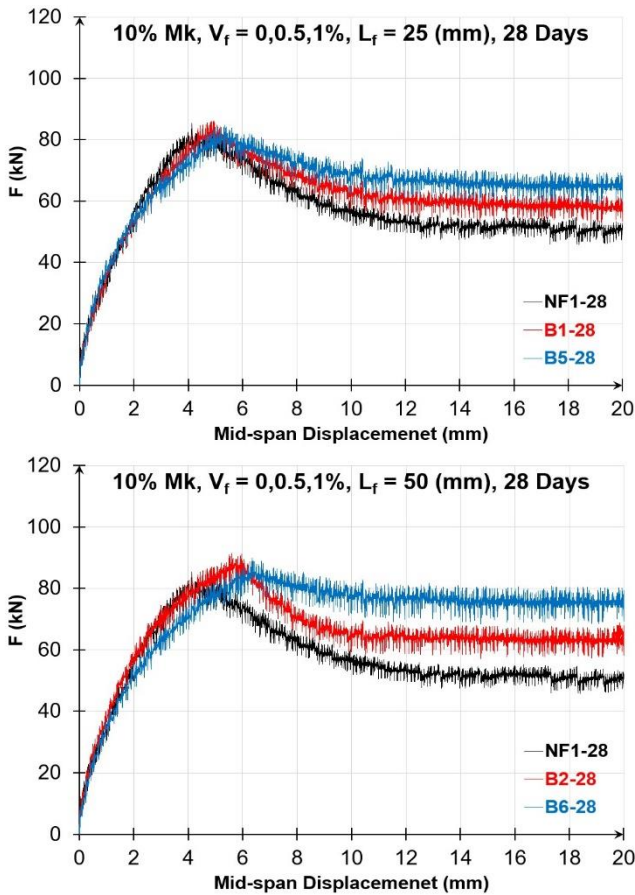


Figure 17. Metakaolin BC beam load-deflection curve

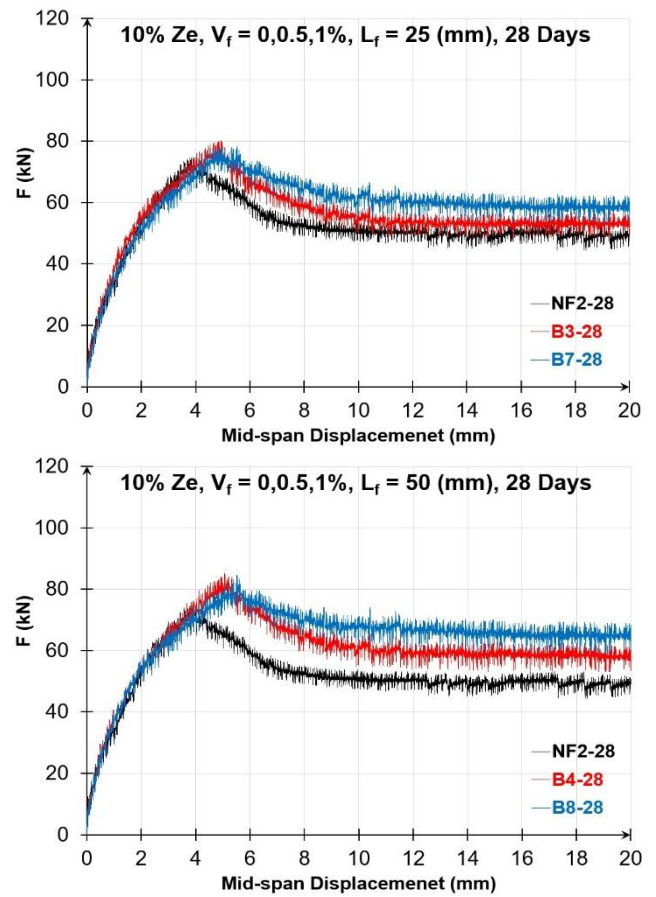


Figure 18. Zeolite BC beam load-deflection curve

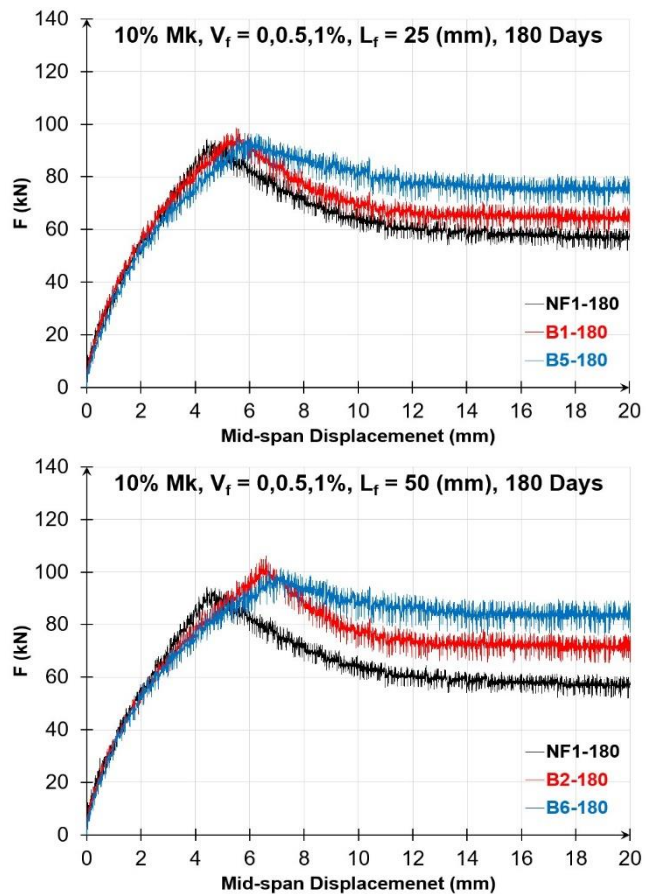


Figure 19. Metakaolin BC beam load-deflection curve

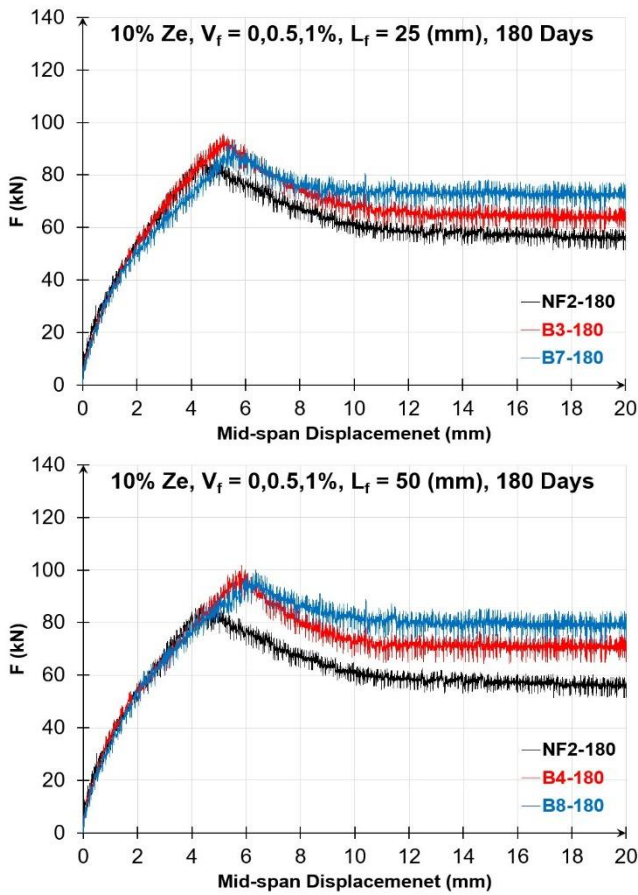


Figure 20. Zeolite BC beam load-deflection curve

4.3.2.1. The BC beams cracking load

In Tables 10-11 and Figure 21, the P_{cr} of the BC beams at 28 and 180 days are shown.

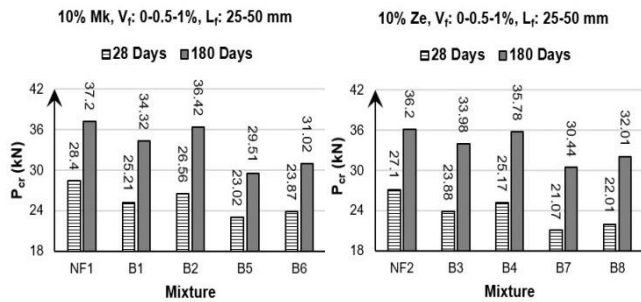


Figure 21. The Cracking load

The P_{cr} of RC beams by adding 0.5 or 1% BF decreased. Furthermore, the P_{cr} of the BC beams was reduced significantly due to the increase in the V_f of BF in the concrete mixtures.

Results revealed that the P_{cr} of the BC beams, which contained 0.5 and 1% BF, exhibited a reduction of up to 11 and 19% as compared to the RC beams, respectively, after 28 days. While the addition of 0.5 and 1% BF resulted in a reduction of P_{cr} in RC beams by 8 and 21%, respectively, at 180 days. In addition, the inclusion of 0.5 and 1% BF in the zeolite RC beams resulted in a reduction of P_{cr} by 12 and 22%, respectively, after 28 days. At 180 days, the P_{cr} of the 0.5 and 1% BC beams exhibited a respective increase of 6 and 16% compared to the RC beams. The

inclusion of BF in mixtures has been observed to result in an augmentation of void space and porosity, ultimately leading to a reduction in the integrity and P_{cr} of specimens [9], [27], [49], [50], [51].

Furthermore, the increase in the A.R. of the BF resulted in a rise in the P_{cr} of BC beams. The increase of P_{cr} for 80 A.R. metakaolin/zeolite BC beams was about 7% more than 40 A.R. ones, at 180 days.

The higher A.R. of BF led to increased bonding length within the cement matrix and greater adhesion compared to the 40 A.R. Consequently, the P_{cr} of the 80 A.R. BC beams was higher than that of the 40 A.R. [9], [27], [33], [49], [50], [51].

Based on the obtained results, the findings suggest that, after 28 days, the P_{cr} of metakaolin BC beams was greater than that of zeolite BC beams. However, at 180 days, the same results were obtained for zeolite and metakaolin mixtures [8], [16], [60]. For instance, at 28 days, metakaolin BC beams with 0.5 and 1% BF exhibited P_{cr} up to 6 and 10% greater than zeolite ones.

4.3.2.2. The BC beams peak load

Table 12 and Figure 22 illustrate the impact of fibers and SCMs, such as metakaolin or zeolite, on the P_{max} .

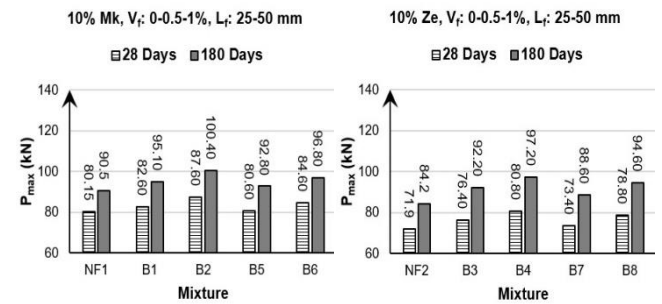


Figure 22. P_{max} of the BC beams

The findings indicated that the P_{max} of the metakaolin/zeolite BC beams was higher than the RC ones. While the GRFC beams containing 1% BF had lower P_{max} than 0.5% BF. The beams containing 0.5 and 1% BF exhibited greater P_{max} at 28 days, with increases of up to 13 and 10% compared to those of RC. Furthermore, at 180 days, the P_{max} increased up to 16 and 13% by adding 0.5 and 1% BF to the metakaolin/zeolite RC beams, respectively. According to extracted results, as the V_f of BF in the mixes increases, there is a parallel rise in hole volume and porosity, while the integrity and P_{max} of RC decrease [9], [27], [49], [50], [51], [54], [61].

Besides, the augmentation of the BF A.R. led to a rise in the P_{max} of the BC beams. The BC beams with an A.R. of 80 exhibited a P_{max} that was approximately 8% greater than that of the beams with an A.R. of 40, at all days. Through the enhancement of BF's length and A.R., cement paste-fiber adhesion, as well as the development length of fibers, and P_{max} , are enhanced [9], [27], [33], [49], [50], [51], [54], [62].

Moreover, considering the results presented in Tables 10 and 12, it is evident that the P_{max} of the metakaolin BC beams surpassed that of the zeolite ones by up to 10 and 5% at 28 and 180 days, respectively.

The results reveal that metakaolin BC beams with finer particle size and higher pozzolanic activity exhibit a greater P_{max} than their zeolite ones at 28 days. However, at 180 days, the completion of the hydration process and the enhancement of microstructure and bond strength lead to a reduction in the disparity between the P_{max} values of metakaolin/zeolite BC beams [8], [16], [60].

4.3.2.3. The BC beams flexural toughness

The T value of RC beams was observed to increase upon the use of BF, as evidenced by the data presented in Figures 17-20 and 23, as well as Tables 10 and 12.

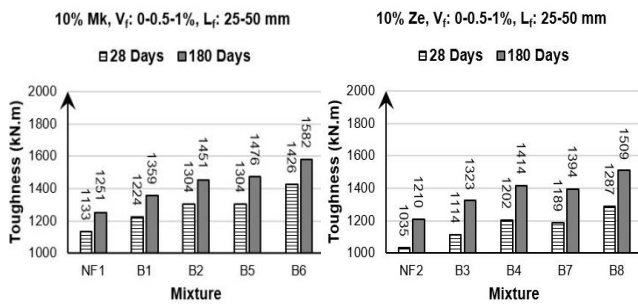


Figure 23. T of the BC beams

Furthermore, by increasing the V_f of BF in BC beams from 0.5 to 1%, the T rose. For instance, the combination of 0.5 and 1% BF to RC beams resulted in an increase in T to 17 and 27% at early and long times, respectively. Also, the 1% BC beams had higher T up to 9% than the 0.5% BC ones. Despite the higher strength of GF compared to BF, the BF has a role in helping to control and distribute loads through the crack bridging. Therefore, the increase of the T will be expected [45], [46], [48], [49], [54], [61], [67], [68], [69].



Figure 24. The BC beams crack bridging

Crack bridging is a fiber performance to delay and prevent from distribution of cracks in the concrete beams. The T and ductility of beams are enhanced by strengthening fiber bridging. Therefore, by augmenting the V_f , more fibers can bear the applied load, so the effectiveness of crack bridging and the T of beams will be risen [23], [48], [49], [53], [70]. The

crack bridging of fibers in BC beams has been illustrated in Figure 24.

According to Table 12 and Figure 23, by changing the A.R. of BF from 40 to 80, the T of the BC beams rose about 10%. It will be expected that the T of BC beams will be enhanced when the A.R. of BF, length, developmental length, adhesion, and fiber pull out resistance from the cement paste is enhanced [9], [27], [49], [50], [51], [54].

After comparing the findings, it was observed that the T of BC beams containing metakaolin surpassed that of BC beams containing zeolite. However, for a long time, it was found that the T of BF beams and metakaolin/zeolite were identical. After 28 days, the T of BC beams with metakaolin exhibited an increase of up to 11% in comparison to the zeolite ones. However, after 180 days, the T of metakaolin BC beams including 0.5% BF was found to be similar to that of the zeolite beams [8], [13], [16], [60].

4.3.3. Comparison of the GC and BC beams

Figures 26-28 demonstrate the P_{cr} , P_{max} , and T of the GC and BC beams with zeolite or metakaolin as SCM, after 180 days.



Figure 25. The cross-section of GC and BC beams

According to the findings displayed in Figure 26 and Table 10, it is apparent that the BC beams' P_{cr} was higher than the GC beams. However, it is notable that the disparity in P_{cr} between the types of beams exhibited an upward trend over time.

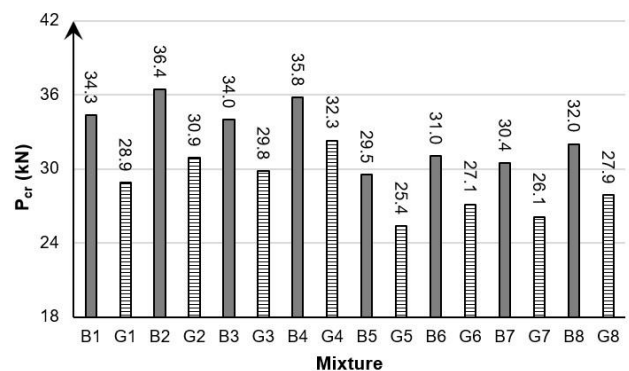


Figure 26. P_{cr} of GC and BC beams (180 days)

To illustrate, at 28 and 180 days, the P_{cr} of BC beams were about 14 and 19% higher than GC beams, respectively. It can be concluded that the greater hardness and inflexibility of GF compared to BF

causes to increase in porosity and decrease the density, integrity, and P_{cr} of GC beams [9], [23], [27], [29], [33], [46], [48], [49], [50], [51], [53], [54], [58], [62].

Furthermore, according to the results of Table 10 and Figures 27-28, it can be determined that in comparison to BC beams, the GC beams had higher P_{max} and T.

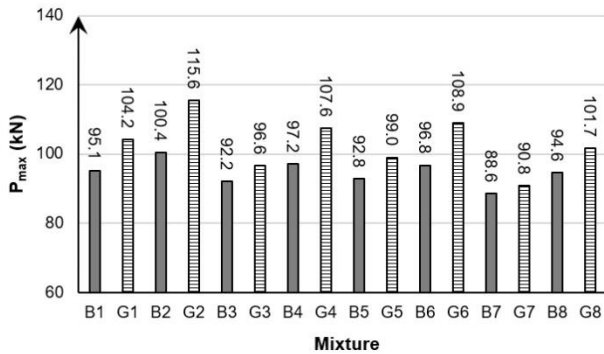


Figure 27. P_{max} of GC and BC beams (180 days)

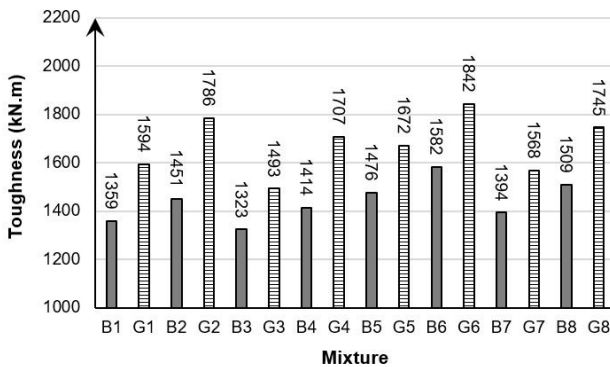


Figure 28. T of GC and BC beams (180 days)

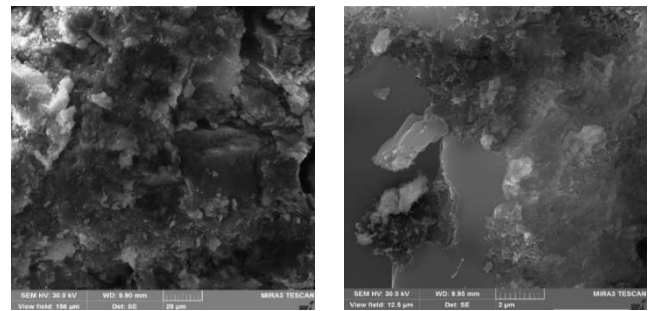
For example, the P_{max} of the GC beams with 0.5 and 1% GF was more than the BC beams up to 16 and 13% at 28 days. Moreover, the T of the 0.5 and 1% GC beams exhibited an increase of up to 23 and 17%, in comparison to the BC beams after 180 days, respectively. It seems that although the flexibility of GF is lower than BF but its higher tensile strength (about 11 times) helps to better control cracking, prevent crack development, better distribute loads, and finally, increase the P_{max} and T of the GC beams [9], [23], [27], [33], [48], [49], [50], [51], [54], [58].

4.4. The scanning electron microscope (SEM)

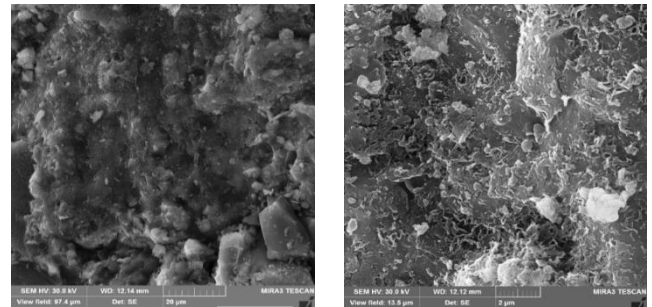
Figure 29 illustrates the SEM analysis of concrete mixes that incorporate metakaolin/zeolite, providing a precise investigation and evaluation of their microstructural characteristics. The samples were prepared by taking small pieces of fiber concrete from cubic specimens (70×70×70 mm) which were coated with thin gold sheets to improve the image quality.

Figure 30 displays the SEMs of the area located between the cement paste and fiber. Furthermore, in Figure 31, the cement hydration products including ettringite, HC, and C-S-H gels are displayed. Also, the

micro/macro pore and cracks in cement paste are demonstrated in Figure 32.



The metakaolin concrete mixture



The zeolite concrete mixture

Figure 29. The microstructural properties of concrete mixtures

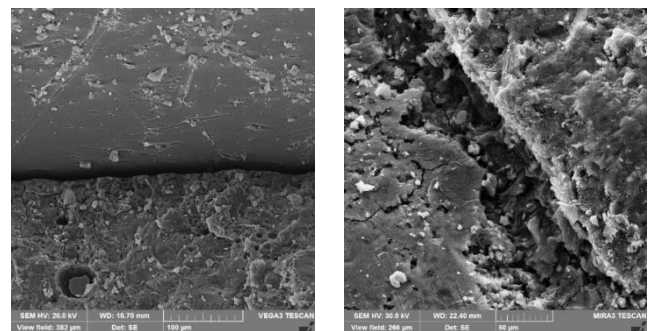


Figure 30. Fiber and cement paste contact zone

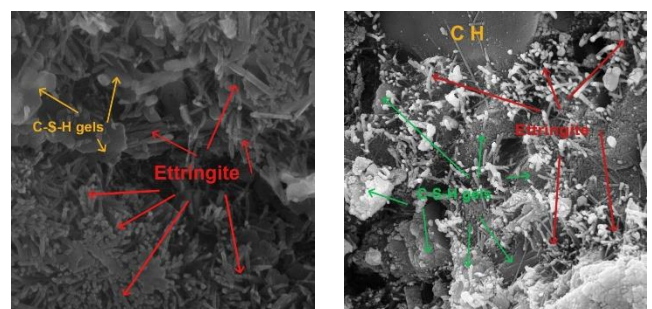


Figure 31. The cement hydration products

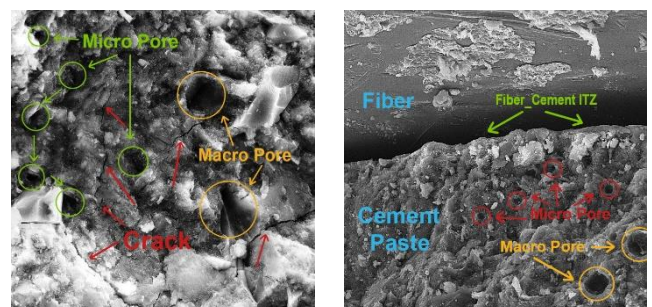


Figure 32. The micro/macro pore and cracks in cement paste

4.5. Cracking behavior

The four-point bending test is utilized for both RC and FRC beams, wherein a load protocol that increases monotonically is applied to the beams. Typically, the first crack in a beam occurs in the tensile zone, specifically on the bottom face. Subsequently, by raising the load, flexural fractures developed from the beams' bottom faces upward. In continuation and with an increase in the load, flexural cracks emerged and extended toward the compressive zone. The initial cracks exhibited greater depth and width. The majority of the flexural cracks manifested in the vicinity of the mid-span beams. The improvement of crack propagation resistance can be achieved by augmenting RC beams with fibers and enhancing the V_f of fibers [31], [71], [72].

The findings suggest a direct correlation between the quantity and attributes of flexural cracks and the fiber type and amount in the concrete mixes. The combination of fibers into the RC beams led to an increase in both primary and secondary cracking. The dimension of cracks like breadth and spacing were also reduced. For instance, according to Figure 30, by adding 1% GF/BF fibers to the RC beams, the number of major and minor cracks were increased. Furthermore, fiber RC beams containing 1% GF/BF fibers had cracks with less width and distance than RC beams.



Figure 33. Measurement of the crack dimensions

Furthermore, elevating the A.R. of GF/BF fibers from 40 to 80 resulted in heightened adhesion of fibers in the cement paste, thereby augmenting the pull-out resistance of fibers. This, in turn, reinforced crack bridging, restricted the distribution of cracks, and reduced the number and width of cracks [26], [63], [67], [73].

For more examination of the crack behavior of RC beams without/with fiber, in Figure 34, the cracking patterns are shown.

As a result, the concurrent utilization of recycled strip fibers (GF/BF) and SCMs such as metakaolin and zeolite, has the potential to mitigate air and marine pollution, restrict crack development, and enhance the ductility of RC beams.

5. Conclusion

The current research aims to evaluate the compressive strength, flexural toughness, flexural behavior, and cracking behavior of RC, GC, and BC beams that incorporated SCM like metakaolin and zeolite. The evaluation was conducted at 28 and 180 days in the Oman Sea's tidal zone. The primary findings are:

1- The incorporation of GF/BF into the concrete mixes led to a reduction of approximately 22% in the f'_c of the concrete specimens. Moreover, it was discovered that the f'_c of concrete containing zeolite was greater than that of metakaolin concrete at an early age.

2- The P_{cr} of fiber RC beams containing GF/BF fibers was up to 32 and 23% lower than RC beams, respectively. In a short time, the fiber RC beams containing metakaolin exhibited a greater P_{cr} by up to 10% compared to those containing zeolite. However, at long term, the P_{cr} of zeolite fiber RC beams was found to be nearly equivalent to that of metakaolin fiber RC beams.

3- The P_{max} of RC beams by adding 0.5% GF and BF decreased by 28 and 16%, at 180 days, respectively, but RC beams containing 1% GF and BF had higher P_{max} than RC beams up to 21 and 13%, respectively.

4- At 28 and 180 days, the GC beams, which were composed of 0.5 and 1% GF, exhibited a greater P_{max} of up to 16 and 13% compared to the BC beams, respectively.

5- The P_{max} of FRC beams containing metakaolin was found to be 13 and 9% greater than those containing zeolite after 28 and 180 days, respectively.

6- The combination of 0.5 or 1% GF in RC beams resulted in an increase in the toughness of the beams up to 43 and 48%, respectively. Moreover, it was observed that the toughness of beams made with BC containing 0.5 or 1% BF was 17 and 27% higher, respectively, compared to RC beams.

7- The toughness of fiber RC beams with 0.5 or 1% GF exhibited an increase of 23 and 17%, respectively, compared to those with BF.

8- The toughness of metakaolin FRC beams was observed to be higher than that of zeolite FRC beams. However, as time goes on, the disparity in their toughness reduced.

9- The propagation of cracks in RC beams was found to be mitigated through the incorporation of GF/BF, as well as an increase in both the V_f and A.R. of fibers. Additionally, it was discovered that there were more cracks than before.



Figure 34. Cracking patterns of GC/BC beams (180 days)

6. References

- [1] M. Valipour, M. Shekarchi, and M. Arezoumandi, 'Chlorine diffusion resistivity of sustainable green concrete in harsh marine environments', *J Clean Prod*, vol. 142, pp. 4092–4100, Jan. 2017, doi: 10.1016/j.jclepro.2016.10.015.
- [2] A. Azad, A. Saeedian, S.-F. Mousavi, H. Karami, S. Farzin, and V. P. Singh, 'Effect of zeolite and pumice powders on the environmental and physical characteristics of green concrete filters', *Constr Build Mater*, vol. 240, p. 117931, Apr. 2020, doi: 10.1016/j.conbuildmat.2019.117931.
- [3] M. Valipour, M. Yekkar, M. Shekarchi, and S. Panahi, 'Environmental assessment of green concrete containing natural zeolite on the global warming index in marine environments', *J Clean Prod*, vol. 65, pp. 418–423, Feb. 2014, doi: 10.1016/j.jclepro.2013.07.055.
- [4] H. Shahrabadi and D. Vafaei, 'Effect of kerosene impacted sand on compressive strength of concrete in different exposure conditions', *Journal of Materials and Environmental Science*, vol. 6, no. 9, 2015.
- [5] M. Najimi, J. Sobhani, B. Ahmadi, and M. Shekarchi, 'An experimental study on durability properties of concrete containing zeolite as a highly reactive natural pozzolan', *Constr Build Mater*, vol. 35, pp. 1023–1033, Oct. 2012, doi: 10.1016/j.conbuildmat.2012.04.038.
- [6] H. Shahrabadi, S. Sayareh, and H. Sarkardeh, 'Effect of silica fume on compressive strength of oil-polluted concrete in different marine environments', *China Ocean Engineering*, vol. 31, no. 6, 2017, doi: 10.1007/s13344-017-0082-6.
- [7] Y. T. Tran, J. Lee, P. Kumar, K.-H. Kim, and S. S. Lee, 'Natural zeolite and its application in concrete composite production', *Compos B Eng*, vol. 165, pp. 354–364, May 2019, doi: 10.1016/j.compositesb.2018.12.084.
- [8] P. Rashiddadash, A. A. Ramezani-pour, and M. Mahdikhani, 'Experimental investigation on flexural toughness of hybrid fiber reinforced concrete (HFRC) containing metakaolin and pumice', *Constr Build Mater*, vol. 51, pp. 313–320, Jan. 2014, doi: 10.1016/j.conbuildmat.2013.10.087.
- [9] P. S. Song, S. Hwang, and B. C. Sheu, 'Strength properties of nylon- and polypropylene-fiber-reinforced concretes', *Cem Concr Res*, vol. 35, no. 8, pp. 1546–1550, Aug. 2005, doi: 10.1016/j.cemconres.2004.06.033.
- [10] D. K. Panesar and R. Zhang, 'Performance comparison of cement replacing materials in concrete: Limestone fillers and supplementary cementing materials – A review', *Constr Build Mater*, vol. 251, p. 118866, Aug. 2020, doi: 10.1016/j.conbuildmat.2020.118866.
- [11] A. M. Rashad, 'Metakaolin as cementitious material: History, scours, production and composition – A comprehensive overview', *Constr Build Mater*, vol. 41, pp. 303–318, Apr. 2013, doi: 10.1016/j.conbuildmat.2012.12.001.
- [12] X. Qian and Z. Li, 'The relationships between stress and strain for high-performance concrete with metakaolin', *Cem Concr Res*, vol. 31, no. 11, pp. 1607–1611, Nov. 2001, doi: 10.1016/S0008-8846(01)00612-3.
- [13] R. Siddique and J. Klaus, 'Influence of metakaolin on the properties of mortar and concrete: A review', *Appl Clay Sci*, vol. 43, no. 3–4, pp. 392–400, Mar. 2009, doi: 10.1016/j.clay.2008.11.007.
- [14] O. R. Kavitha, V. M. Shanthi, G. Prince Arulraj, and P. Sivakumar, 'Fresh, micro- and macrolevel studies of metakaolin blended self-compacting concrete', *Appl Clay Sci*, vol. 114, pp. 370–374, Sep. 2015, doi: 10.1016/j.clay.2015.06.024.
- [15] V. Punitha, N. Sakthieswaran, and O. Ganesh Babu, 'Experimental investigation of concrete incorporating HDPE plastic waste and metakaolin', *Mater Today Proc*, no. xxxx, Jul. 2020, doi: 10.1016/j.matpr.2020.06.288.
- [16] F. A. Sabet, N. A. Libre, and M. Shekarchi, 'Mechanical and durability properties of self consolidating high performance concrete incorporating natural zeolite, silica fume and fly ash', *Constr Build Mater*, vol. 44, pp. 175–184, Jul. 2013, doi: 10.1016/j.conbuildmat.2013.02.069.
- [17] K. Samimi, S. Kamali-Bernard, and A. A. Maghsoudi, 'Durability of self-compacting concrete containing pumice and zeolite against acid attack, carbonation and marine environment', *Constr Build Mater*, vol. 165, pp. 247–263, Mar. 2018, doi: 10.1016/j.conbuildmat.2017.12.235.
- [18] H. Shahrabadi, S. Sayareh, and H. Sarkardeh, 'Effect of Natural Zeolite-Pozzolan on Compressive Strength of Oil-Polluted Concrete Marine Structures', *Civil Engineering Journal*, vol. 2, no. 12, p. 623, Feb. 2018, doi: 10.28991/cej-030985.
- [19] E. Emam and S. Yehia, 'Performance of concrete containing zeolite as a supplementary cementitious material', *Int. Res. J. Eng. Technol*, vol. 4, no. 12, pp. 1619–

- 1625, 2017, [Online]. Available: <https://www.irjet.net/archives/V4/i12/IRJET-V4I12297.pdf>
- [20] M. C. G. Juenger and R. Siddique, 'Recent advances in understanding the role of supplementary cementitious materials in concrete', *Cem Concr Res*, vol. 78, pp. 71–80, Dec. 2015, doi: 10.1016/j.cemconres.2015.03.018.
- [21] S. Mehdipour *et al.*, 'Mechanical properties, durability and environmental evaluation of rubberized concrete incorporating steel fiber and metakaolin at elevated temperatures', *J Clean Prod*, vol. 254, p. 120126, May 2020, doi: 10.1016/j.jclepro.2020.120126.
- [22] L. Kan, L. Zhang, Y. Zhao, and M. Wu, 'Properties of polyvinyl alcohol fiber reinforced fly ash based Engineered Geopolymer Composites with zeolite replacement', *Constr Build Mater*, vol. 231, p. 117161, Jan. 2020, doi: 10.1016/j.conbuildmat.2019.117161.
- [23] D. Foti, 'Preliminary analysis of concrete reinforced with waste bottles PET fibers', *Constr Build Mater*, vol. 25, no. 4, pp. 1906–1915, Apr. 2011, doi: 10.1016/j.conbuildmat.2010.11.066.
- [24] M. Zaroudi, R. Madandoust, and K. Aghaee, 'Fresh and hardened properties of an eco-friendly fiber reinforced self-consolidated concrete composed of polyolefin fiber and natural zeolite', *Constr Build Mater*, vol. 241, p. 118064, Apr. 2020, doi: 10.1016/j.conbuildmat.2020.118064.
- [25] O. B. Ozger *et al.*, 'Effect of nylon fibres on mechanical and thermal properties of hardened concrete for energy storage systems', *Mater Des*, vol. 51, pp. 989–997, Oct. 2013, doi: 10.1016/j.matdes.2013.04.085.
- [26] S. B. Kim, N. H. Yi, H. Y. Kim, J.-H. J. Kim, and Y.-C. Song, 'Material and structural performance evaluation of recycled PET fiber reinforced concrete', *Cem Concr Compos*, vol. 32, no. 3, pp. 232–240, Mar. 2010, doi: 10.1016/j.cemconcomp.2009.11.002.
- [27] S. P. Yap, U. J. Alengaram, and M. Z. Jumaat, 'Enhancement of mechanical properties in polypropylene- and nylon-fibre reinforced oil palm shell concrete', *Mater Des*, vol. 49, pp. 1034–1041, Aug. 2013, doi: 10.1016/j.matdes.2013.02.070.
- [28] A. Q. Ahdal *et al.*, 'Mechanical performance and feasibility analysis of green concrete prepared with local natural zeolite and waste PET plastic fibers as cement replacements', *Case Studies in Construction Materials*, vol. 17, no. June, p. e01256, Dec. 2022, doi: 10.1016/j.cscm.2022.e01256.
- [29] H. Alabduljabbar, H. Mohammadhosseini, M. Md. Tahir, and R. Alyousef, 'Green and sustainable concrete production using carpet fibers waste and palm oil fuel ash', *Mater Today Proc*, vol. 39, pp. 929–934, 2021, doi: 10.1016/j.matpr.2020.04.047.
- [30] A. H. Alani, N. M. Bunnori, A. T. Noaman, and T. A. Majid, 'Durability performance of a novel ultra-high-performance PET green concrete (UHPPGC)', *Constr Build Mater*, vol. 209, pp. 395–405, Jun. 2019, doi: 10.1016/j.conbuildmat.2019.03.088.
- [31] M. Shayanfar and H. Shahrabadi, 'Flexural behavior of green RC beams with disposable glasses fibers in a marine environment', *Case Studies in Construction Materials*, vol. 18, p. e01972, Jul. 2023, doi: 10.1016/j.cscm.2023.e01972.
- [32] ASTM International, 'ASTM C136, Standard Test Method for Sieve Analysis of Fine and Coarse Aggregates.', West Conshohocken, PA, 2001. doi: 10.1520/C0136_C0136M-19.
- [33] A. Meza and S. Siddique, 'Effect of aspect ratio and dosage on the flexural response of FRC with recycled fiber', *Constr Build Mater*, vol. 213, pp. 286–291, Jul. 2019, doi: 10.1016/j.conbuildmat.2019.04.081.
- [34] ACI, 'ACI 360R-10, Guide to Design of Slabs-on-Ground', 2010.
- [35] British Standard, 'British Standard BS-EN-12390-3-2009 Testing Hardened Concrete Part 3: Compressive Strength of Test Specimens', London, England, 2009. [Online]. Available: <https://shop.bsigroup.com/ProductDetail/?pid=000000000030253049>
- [36] ASTM International, 'ASTM C78-08, Standard Test Method for Flexural Strength of Concrete (Using Simple Beam with Third-Point Loading)', West Conshohocken, PA, 2008. doi: 10.1520/C0078-08.
- [37] G. Rojo-López, B. González-Fonteboa, F. Martínez-Abella, and I. González-Taboada, 'Rheology, durability, and mechanical performance of sustainable self-compacting concrete with metakaolin and limestone filler', *Case Studies in Construction Materials*, vol. 17, no. May, p. e01143, Dec. 2022, doi: 10.1016/j.cscm.2022.e01143.
- [38] M. Amran *et al.*, 'Properties and performance of polypropylene fibered high-strength concrete with an improved composite binders', *Case Studies in Construction Materials*, vol. 17, no. August, p. e01621, Dec. 2022, doi: 10.1016/j.cscm.2022.e01621.
- [39] J. J. Chen, L. G. Li, P. L. Ng, and A. K. H. Kwan, 'Effects of superfine zeolite on strength, flowability and cohesiveness of cementitious paste', *Cem Concr Compos*, vol.

- 83, pp. 101–110, Oct. 2017, doi: 10.1016/j.cemconcomp.2017.06.010.
- [40] M. Abdellatif, S. M. AL-Tam, W. E. Elemam, H. Alanazi, G. M. Elgendy, and A. M. Tahwia, 'Development of ultra-high-performance concrete with low environmental impact integrated with metakaolin and industrial wastes', *Case Studies in Construction Materials*, vol. 18, no. August 2022, p. e01724, Jul. 2023, doi: 10.1016/j.cscm.2022.e01724.
- [41] N. Saboo, S. Shivhare, K. K. Kori, and A. K. Chandrappa, 'Effect of fly ash and metakaolin on pervious concrete properties', *Constr Build Mater*, vol. 223, pp. 322–328, Oct. 2019, doi: 10.1016/j.conbuildmat.2019.06.185.
- [42] L. Gu and T. Ozbakkaloglu, 'Use of recycled plastics in concrete: A critical review', *Waste Management*, vol. 51, pp. 19–42, May 2016, doi: 10.1016/j.wasman.2016.03.005.
- [43] F. Fraternali, S. Spadea, and V. P. Berardi, 'Effects of recycled PET fibres on the mechanical properties and seawater curing of Portland cement-based concretes', *Constr Build Mater*, vol. 61, pp. 293–302, Jun. 2014, doi: 10.1016/j.conbuildmat.2014.03.019.
- [44] R. Merli, M. Preziosi, A. Acampora, M. C. Lucchetti, and E. Petrucci, 'Recycled fibers in reinforced concrete: A systematic literature review', *J Clean Prod*, vol. 248, p. 119207, Mar. 2020, doi: 10.1016/j.jclepro.2019.119207.
- [45] H. Safayenikoo, 'Metalized Plastic Waste Fiber Effects on Green Concrete Beams Mechanical Performance', *Shock and Vibration*, vol. 2022, pp. 1–15, May 2022, doi: 10.1155/2022/3113841.
- [46] A. Meena, A. Surendranath, and P. V. Ramana, 'Assessment of mechanical properties and workability for polyethylene terephthalate fiber reinforced concrete', *Mater Today Proc*, vol. 50, pp. 2307–2314, 2022, doi: 10.1016/j.matpr.2021.10.054.
- [47] Z. Z. Ismail and E. A. AL-Hashmi, 'Use of waste plastic in concrete mixture as aggregate replacement', *Waste Management*, vol. 28, no. 11, pp. 2041–2047, Nov. 2008, doi: 10.1016/j.wasman.2007.08.023.
- [48] R. Sharma and P. P. Bansal, 'Use of different forms of waste plastic in concrete – a review', *J Clean Prod*, vol. 112, pp. 473–482, Jan. 2016, doi: 10.1016/j.jclepro.2015.08.042.
- [49] Y. Ghernouti, B. Rabehi, T. Bouziani, H. Ghezraoui, and A. Makhloufi, 'Fresh and hardened properties of self-compacting concrete containing plastic bag waste fibers (WFSCC)', *Constr Build Mater*, vol. 82, pp. 89–100, May 2015, doi: 10.1016/j.conbuildmat.2015.02.059.
- [50] A. Zia and M. Ali, 'Behavior of fiber reinforced concrete for controlling the rate of cracking in canal-lining', *Constr Build Mater*, vol. 155, pp. 726–739, Nov. 2017, doi: 10.1016/j.conbuildmat.2017.08.078.
- [51] Y. Qin, X. Zhang, and J. Chai, 'Damage performance and compressive behavior of early-age green concrete with recycled nylon fiber fabric under an axial load', *Constr Build Mater*, vol. 209, pp. 105–114, Jun. 2019, doi: 10.1016/j.conbuildmat.2019.03.094.
- [52] B. Ali, M. Fahad, A. S. Mohammed, H. Ahmed, A. B. Elhag, and M. Azab, 'Improving the performance of recycled aggregate concrete using nylon waste fibers', *Case Studies in Construction Materials*, vol. 17, no. July, p. e01468, Dec. 2022, doi: 10.1016/j.cscm.2022.e01468.
- [53] S. Ullah Khan and T. Ayub, 'Flexure and shear behaviour of self-compacting reinforced concrete beams with polyethylene terephthalate fibres and strips', *Structures*, vol. 25, no. December 2019, pp. 200–211, Jun. 2020, doi: 10.1016/j.istruc.2020.02.023.
- [54] M. Kumaresan, S. Sindhu Nachiar, and S. Anandh, 'Implementation of waste recycled fibers in concrete: a review', *Mater Today Proc*, vol. 68, pp. 1988–1994, 2022, doi: 10.1016/j.matpr.2022.08.228.
- [55] N. K. Bui, T. Satomi, and H. Takahashi, 'Recycling woven plastic sack waste and PET bottle waste as fiber in recycled aggregate concrete: An experimental study', *Waste Management*, vol. 78, pp. 79–93, Aug. 2018, doi: 10.1016/j.wasman.2018.05.035.
- [56] H. K. Shehab El-Din, A. S. Eisa, B. H. Abdel Aziz, and A. Ibrahim, 'Mechanical performance of high strength concrete made from high volume of Metakaolin and hybrid fibers', *Constr Build Mater*, vol. 140, pp. 203–209, Jun. 2017, doi: 10.1016/j.conbuildmat.2017.02.118.
- [57] M. Valipour, F. Pargar, M. Shekarchi, and S. Khani, 'Comparing a natural pozzolan, zeolite, to metakaolin and silica fume in terms of their effect on the durability characteristics of concrete: A laboratory study', *Constr Build Mater*, vol. 41, pp. 879–888, Apr. 2013, doi: 10.1016/j.conbuildmat.2012.11.054.
- [58] F. S. Khalid, J. M. Irwan, M. H. W. Ibrahim, N. Othman, and S. Shahidan, 'Performance of plastic wastes in fiber-reinforced concrete beams', *Constr Build Mater*, vol. 183, pp. 451–464, Sep. 2018, doi: 10.1016/j.conbuildmat.2018.06.122.
- [59] H. M. Adnan and A. O. Dawood, 'Strength behavior of reinforced concrete beam using re-cycle of PET wastes as synthetic fibers', *Case Studies in Construction Materials*, vol.

- 13, p. e00367, Dec. 2020, doi: 10.1016/j.cscm.2020.e00367.
- [60] A. Jain, N. Sharma, R. Choudhary, R. Gupta, and S. Chaudhary, 'Utilization of non-metalized plastic bag fibers along with fly ash in concrete', *Constr Build Mater*, vol. 291, p. 123329, Jul. 2021, doi: 10.1016/j.conbuildmat.2021.123329.
- [61] S. Spadea, I. Farina, A. Carrafiello, and F. Fraternali, 'Recycled nylon fibers as cement mortar reinforcement', *Constr Build Mater*, vol. 80, pp. 200–209, Apr. 2015, doi: 10.1016/j.conbuildmat.2015.01.075.
- [62] R. Alyousef, H. Mohammadhosseini, M. Md. Tahir, and H. Alabduljabbar, 'Green concrete composites production comprising metalized plastic waste fibers and palm oil fuel ash', *Mater Today Proc*, no. xxxx, Apr. 2020, doi: 10.1016/j.matpr.2020.04.023.
- [63] A. C. Bhogayata and N. K. Arora, 'Fresh and strength properties of concrete reinforced with metalized plastic waste fibers', *Constr Build Mater*, vol. 146, pp. 455–463, Aug. 2017, doi: 10.1016/j.conbuildmat.2017.04.095.
- [64] M. A. Farooq, M. Fahad, B. Ali, S. Ullah, M. H. El Ouni, and A. B. Elhag, 'Influence of nylon fibers recycled from the scrap brushes on the properties of concrete: Valorization of plastic waste in concrete', *Case Studies in Construction Materials*, vol. 16, no. March, p. e01089, Jun. 2022, doi: 10.1016/j.cscm.2022.e01089.
- [65] I. H. Alfahdawi, S. A. Osman, R. Hamid, and A. I. AL-Hadithi, 'Influence of PET wastes on the environment and high strength concrete properties exposed to high temperatures', *Constr Build Mater*, vol. 225, pp. 358–370, Nov. 2019, doi: 10.1016/j.conbuildmat.2019.07.214.
- [66] R. H. Faraj, H. F. Hama Ali, A. F. H. Sherwani, B. R. Hassan, and H. Karim, 'Use of recycled plastic in self-compacting concrete: A comprehensive review on fresh and mechanical properties', *Journal of Building Engineering*, vol. 30, p. 101283, Jul. 2020, doi: 10.1016/j.job.2020.101283.
- [67] F. Pacheco-Torgal, Y. Ding, and S. Jalali, 'Properties and durability of concrete containing polymeric wastes (tyre rubber and polyethylene terephthalate bottles): An overview', *Constr Build Mater*, vol. 30, pp. 714–724, May 2012, doi: 10.1016/j.conbuildmat.2011.11.047.
- [68] A. H. Alani, M. Azmi Megat Johari, A. Tareq Noaman, N. Muhamad Bunnori, and T. A. Majid, 'Effect of the incorporation of PET fiber and ternary blended binder on the flexural and tensile behaviour of ultra-high performance green concrete', *Constr Build Mater*, vol. 331, no. August 2021, p. 127306, May 2022, doi: 10.1016/j.conbuildmat.2022.127306.
- [69] N. Z. Nkomo, L. M. Masu, and P. K. Nziu, 'Optimisation of mechanical properties of polyethylene terephthalate fibre/fly ash hybrid concrete composite', *Case Studies in Construction Materials*, vol. 17, no. July, p. e01395, Dec. 2022, doi: 10.1016/j.cscm.2022.e01395.
- [70] F. S. Khalid, J. M. Irwan, M. H. Wan Ibrahim, N. Othman, and S. Shahidan, 'Splitting tensile and pullout behavior of synthetic wastes as fiber-reinforced concrete', *Constr Build Mater*, vol. 171, pp. 54–64, May 2018, doi: 10.1016/j.conbuildmat.2018.03.122.
- [71] W. Alnahhal and O. Aljidda, 'Flexural behavior of basalt fiber reinforced concrete beams with recycled concrete coarse aggregates', *Constr Build Mater*, vol. 169, pp. 165–178, 2018, doi: 10.1016/j.conbuildmat.2018.02.135.
- [72] H. C. Mertol, E. Baran, and H. J. Bello, 'Flexural behavior of lightly and heavily reinforced steel fiber concrete beams', *Constr Build Mater*, vol. 98, pp. 185–193, Nov. 2015, doi: 10.1016/j.conbuildmat.2015.08.032.
- [73] S. Y. Al-Darzi, 'The effect of using shredded plastic on the behavior of reinforced concrete slab', *Case Studies in Construction Materials*, vol. 17, no. November, p. e01681, Dec. 2022, doi: 10.1016/j.cscm.2022.e01681.